



A Headphone-Based Heart Rate and Heart Rate Variability Monitoring Unit

Gashaye Lewtie Hailu^(✉)

Bahir Dar Institute of Technology, Bahir Dar University, Bahir Dar, Ethiopia
gashay2009@gmail.com

Abstract. The Heart Rate (HR) is detected using the Reflectance Photoplethysmography (PPG) Technique, which is a non-invasive approach for measuring changes in blood volume in tissue using an appropriate light source and detector. This study presents a new headphone-based Heart Rate and Heart Rate Variability (HRV) monitoring device. The system is portable and built into conventional headphones. Because the device is built into the headphone, the HR and HRV are recorded without causing any disruption or inconvenience to the person wearing it. The captured data is wirelessly transferred to and displayed on a cell phone through Bluetooth communication. In this work, an android interface was developed and used to show data obtained in the form of beats per minute (BPM) using the MIT App Inventor 2 Bluetooth connectivity application. The device is powered by 5 V by the Intex Wireless Roaming Headset, which contains two AAA batteries that provide 1.5 V each. Because the headphone only provides 3 V, we need a DC-DC Boost Converter Step Up Module 1–5 V to 5 V 500 mA to provide the appropriate supply voltage to the system. Tests on various persons utilizing the prototype system built demonstrated the scheme's usefulness. Data from eight friends were used in the assessment study. The accuracy of the heart rate measuring device was evaluated with -0.5 ± 2.13 BPM as a tolerance during the normal resting period using the standard device “WEAL Pulse Oximeter Fingertip” manufactured by WEAL.

Keywords: Photoplethysmography (PPG) · Pulse rate · Reflectance · Transmittance · Massachusetts Institute of Technology (MIT) App inventor · Infrared sensor · Signal conditioning circuit · Filters

1 Introduction

Heart rate describes the number of heartbeats per minute [1–4]. However, the beat of a healthy heart is not regular [4]. Fluctuations in the time intervals of adjacent heartbeats are referred to as heart rate variability (HRV) [4]. Measuring heart rate variability (HRV) can help determine the autonomic nervous system's functioning and the ratio of sympathetic and parasympathetic activity [2]. To assist us in adjusting to environmental and psychological difficulties, HRV is an emergent trait of interdependent regulatory systems that function on various time scales [3]. The regulation of autonomic balance,

blood pressure (BP), gas exchange, gut, heart, and vascular tone the size of the blood vessels that control BP are all reflected in HRV. It may also represent the modulation of facial muscles [4].

Noninvasive wearable heart rate monitoring units have recently been used for real-time distant and uninterrupted medical monitoring, owing to a large number of benefits for both physicians and patients through medium- and long-term recording of health indicators during daily life activities [5]. The measurement of heart rate (HR) and heart rate variability (HRV) is an important aspect of any person's cardiovascular health [5–8]. The traditional way of measuring heart rate is to physically place fingers or thumbs over the wrist to detect the arterial pulse [8]. In this method, the felt pulse is counted for one minute, and the number of beats per minute (BPM) is roughly calculated or assessed [8]. However, this strategy is unsuitable for continual inspection [9, 10].

According to [5, 11], ECGs are often recorded using torso-mounted, disposable adhesive electrodes. ECG signals may be distorted during long-term acquisitions during the wearing subject's typical activities as a result of sweat, contact, or movement artifacts [4, 5, 12]. When electrodes are affixed to their skin, people may feel uneasy and exhibit very little compliance. Drying the electrode-applied conductive gel and allergy reactions may affect the time-dependent results. Standard electrode placement necessitates a skilled operator because improper electrode location could lead to a flawed recording.

Photoplethysmography (PPG) has been developed as an alternative method for measuring HRV through the surrogate monitoring of pulse rate variability to address some of these issues and to promote the dissemination of portable and easily wearable devices (PRV) [5]. Due to the high signal amplitude that may be achieved in comparison to other sites, PPG sensors are usually placed on the fingers because the high signal amplitude on the fingertip can be accomplished compared with other body surfaces [8, 9]. According to [10], this arrangement is not appropriate for continuous measuring in daily activities involving the use of the fingers.

The utilization of downsizing technologies, as well as the integration of a PPG sensor, microcontroller, Bluetooth, and DC-DC converter incorporated into headphones near the ear, can help to eliminate motion artifacts caused by torsion or contact. PPG sensors and devices are non-invasive since they have no electrical interaction with the human body [13]. They are also less expensive and require less maintenance than ECG equipment.

A method of measuring blood volume variations caused by the pulsing of blood that occurs with each heartbeat is called plethysmography. Small, wearable pulse rate sensors have been created using photoplethysmography (PPG) technology [14]. These gadgets, made of infrared light-emitting diodes (LEDs) and photodetectors, provide a straightforward, dependable, and affordable method of noninvasively measuring the pulse rate [11, 16]. PPG uses sturdy, low-maintenance optical sensors that are reasonably priced [11]. In this study, it is the perfect portable device because it uses very little power and can be supplied by a battery pack with a 5 V power supply.

From the PPG signal, a variety of clinically important characteristics can be extracted, including heart rate, respiratory rate, respiratory-induced intensity variations (RIIV), ventilatory volumes, and autonomic dysfunction [15].

The most basic PPG sensor comprises an infrared LED and a photodetector that is housed inside the same plastic housing in Fig. 1 [15]. The sensor is attached to the

surface of the body using items such as headphones, earbuds, eyeglasses, etc. The sensor can be either a reflecting or a transmitting kind, as indicated in the figure below.

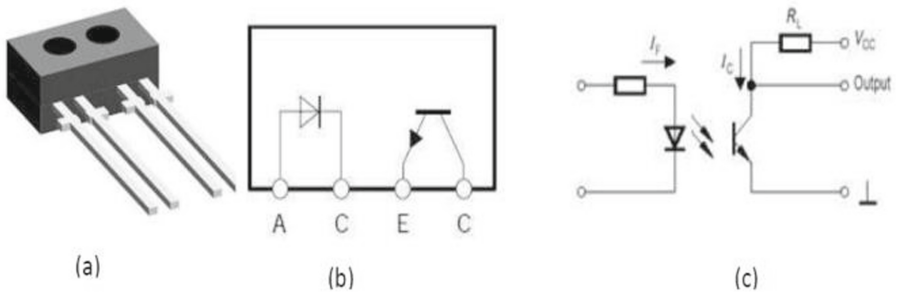


Fig. 1. Reflective optical sensor with transistor output (TCRT1000). (a) TCRT1000 IC; (b) TCRT1000 symbol; (c) TCRT1000 circuit.

In this study, the low-cost, non-intrusive Heart Rate (HR) Monitoring System with Headphones contains a Bluetooth interface that links to the microcontroller is designed, which shows the pulse rate on an Android mobile. The maximum and minimum beat rates per minute are displayed if the monitoring device is connected to the Android phone via an app written using App Inventor 2. Everyone nowadays has access to a home environment where they can monitor and study their heart rate.

The user is free to concentrate solely on exercising with his or her Android phone while running, driving, biking, or performing another activity without having to constantly check their heart rate. This improved form of exercise is shaping the future of driving, training, and exercise because the gadget is less expensive, portable, and safe than constantly monitoring yourself. Additionally, it reflects several physiological states such as biological workload, stress at work, and attention to tasks, as well as the autonomic nervous system's active state.

The number of heartbeats in total that take place over the course of a minute is referred to as heart rate. However, Heart rate variability (HRV) is the term used to describe the normal variation in heart rate that takes place throughout time as shown in Table 2. The variation in the peak-to-peak interval is used to calculate it. Calculate the heart rate for each beat as illustrated in (Fig. 2) below by using the LabView oscilloscope to measure the interval between peaks of a PPG signal. The oscilloscope's time per division is set to 200 ms. We can calculate the heart rate variability using the PPG graph in Fig. 2 below using time domain analysis.

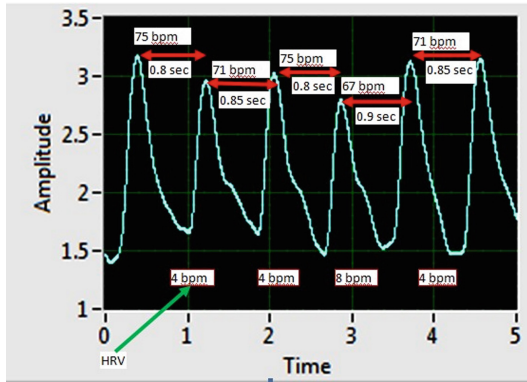


Fig. 2. Heart rate variability from PPG signal

Heart rate variability time-domain indices assess the amount of HRV detected over monitoring periods ranging from 1 min to 24 h [16]. The variation of beat-to-beat intervals, also known as R-R intervals, is referred to as HRV [7]. The average heart rate variability is expressed using the standard deviation of all RR intervals [7]:

$$HRV = \sqrt{\frac{\sum_{i=1}^N (RR_i - \overline{RR})^2}{N - 1}}$$

2 Materials and Methods

The volunteer’s eight healthy friends took part in the study, in which they were monitored using wearable devices while performing various activities. The proposed system components are integrated with the headphone, as shown in Fig. 3 below.

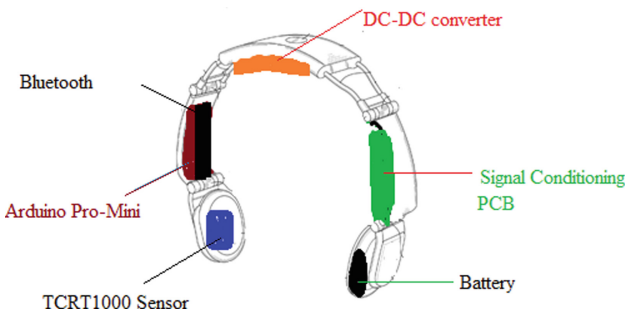


Fig. 3. The position of the system’s components on the headphones is suggested.

The integrated components in Fig. 3 include the battery, sensor, signal conditioning circuit, Bluetooth, Arduino pro-mini, and DC-DC step-up converter.

2.1 General Block Diagram of the Proposed System

The general block design of the proposed system's hardware is depicted in Fig. 4 and uses reflecting photoplethysmography (PPG) to measure heart rate and heart rate variability through headphones. The PPG signal is made up of a large DC component as well as a pulsatile (AC) component. The AC component, which contains vital information such as heart rate, is much weaker than the DC component, and the PPG signal from the phototransistor is weak and noisy. To obtain a photoplethysmograph (PPG) signal, we need an amplifier and filter circuits to boost and clean the signal. The Arduino pro-mini board, which is used for signal processing, is the heart of the project and is responsible for all of the major digitalization of the PPG signal and beat rate calculation. The average heart rate in one minute is calculated using an Arduino pro-mini microcontroller, and the beat per minute is displayed on an Android phone via Bluetooth communication. If someone wants to use the LCD instead of the Android phone display, there is another display system in this device.

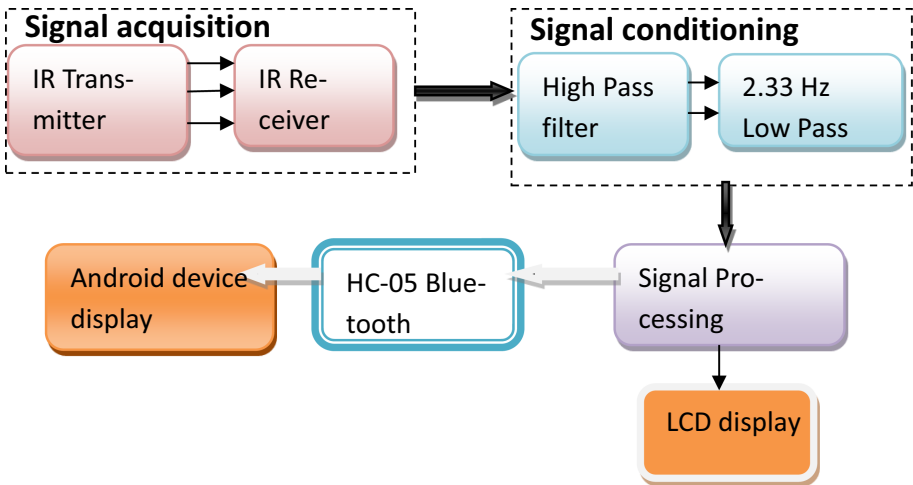


Fig. 4. The block diagram of the system

2.2 The Sensor Output Signal

The output voltage from the phototransistor without a filtering circuit consists of the pulsatile AC signal and slow varying high DC voltage. The output waveform of the sensor is shown below on different surfaces of the body.

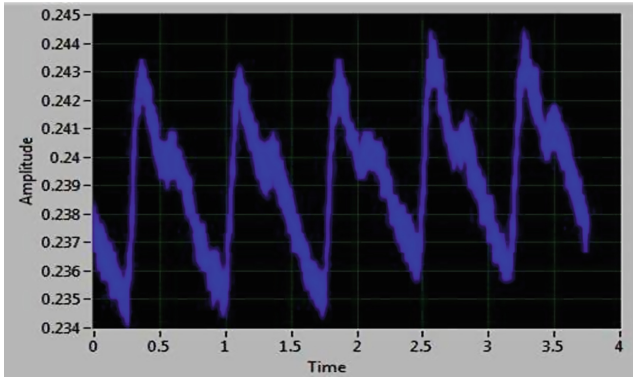


Fig. 5. Signal from a fingertip sensor output

Comparing the PPG signal without a signal conditioning circuit, from the sensor to other body surfaces depicted in Fig. 5 above, the AC signal is considerably high and the DC voltage is low and slowly fluctuating.

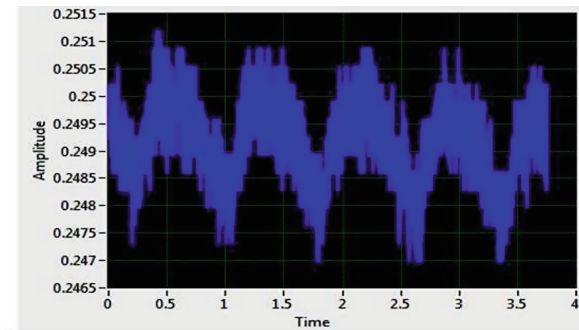


Fig. 6. Near-ear surface sensor output signal

The output signal from the sensor placed close to the ear is depicted in Fig. 6 above. In comparison to the sensor placed on the fingertip, the slow-varying DC voltage is larger and the AC signal is lower. We can get rid of the AC signal and slowly vary the DC voltage by using a signal conditioning circuit.

2.3 Signal Conditioning

The two-stage signal condition circuits are used to eliminate unwanted signals. High-pass filter and low-pass filter circuits are cascaded in the first-stage and second-stage signal conditioning circuits. The high pass signal conditioning circuit produces the necessary information, which will smother the significant DC component from the sensor. The HPF's cut-off frequency is set at 0.5 Hz. The high pass filter's cut-off frequency is determined by the resistor R1 and capacitor C1, as shown in Fig. 8. However, low

pass signal conditioning will eliminate the significant DC component and enhance the weak pulsatile AC component, which conveys the necessary data. The cut-off frequency is determined by the resistor R2 and capacitor C2 as indicated in Fig. 8. The cutoff frequency in the circuit above was set to roughly 2.33 kHz, which corresponded to a maximum heart rate of 140 bpm. To achieve this, we used a resistor R2 of value 680 k and a capacitor C2 of value 100 nF.

As depicted in Fig. 7, the PPG output signal from the first stage signal conditioning circuit contains a low, slowly fluctuating DC voltage and a high AC signal.

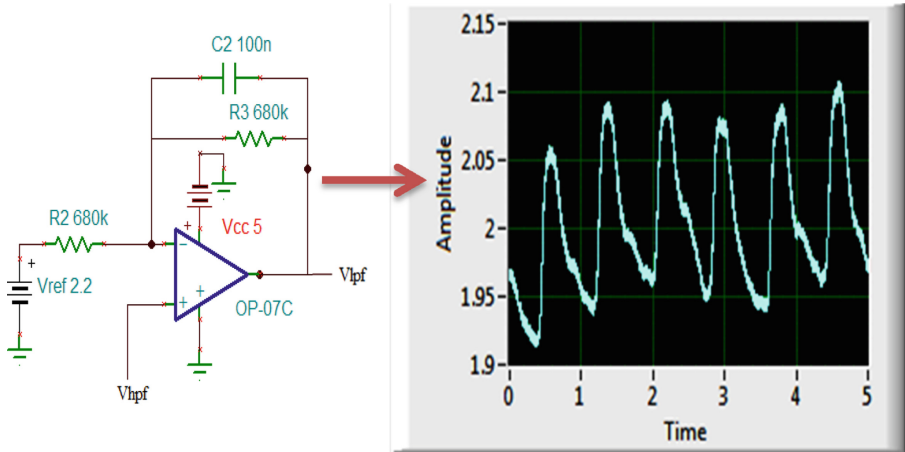


Fig. 7. PPG signal from the first stage of signal conditioning

The output signal from the first signal conditioning stage is not a pure sinusoidal waveform and is too faint to be used for beat calculation. As a result, HPF/LPF is employed for additional filtering and amplification in the second stage. The Second Stage high pass circuit, which is essentially a replica of the First Stage circuit, now receives the output from the active Low Pass Filter.

Similar HPF and varied gains from the first stage LPF circuits are also present in the second stage. A second Op-amp that is set up as a non-inverting buffer with G2 gain is now fed the two-step amplified and filtered signal. The necessary analog PPG signal is provided at the output of the second step. The PPG signal's amplitude, which is visible in the second stage's output, can be managed using the Gain G2.

Therefore, the two cascaded stages' combined voltage gain is $G = G1 * G2 = 101 * 20.4 = 2063.28$. Beats per minute (BPM) = $60 * f$, which is the relationship between the frequency (f) of these pulses and heart rate (BPM).

2.5 Data Acquisition System

The workspace for the initial design and development of the hardware was NI ELVIS, and DAQ from LABVIEW was utilized for signal conditioning with a band-pass filter block and computer-based output signal display. Before being used by the signal conditioning circuit, the sensor's output signal is digitally filtered using the filter express VI from LABVIEW.

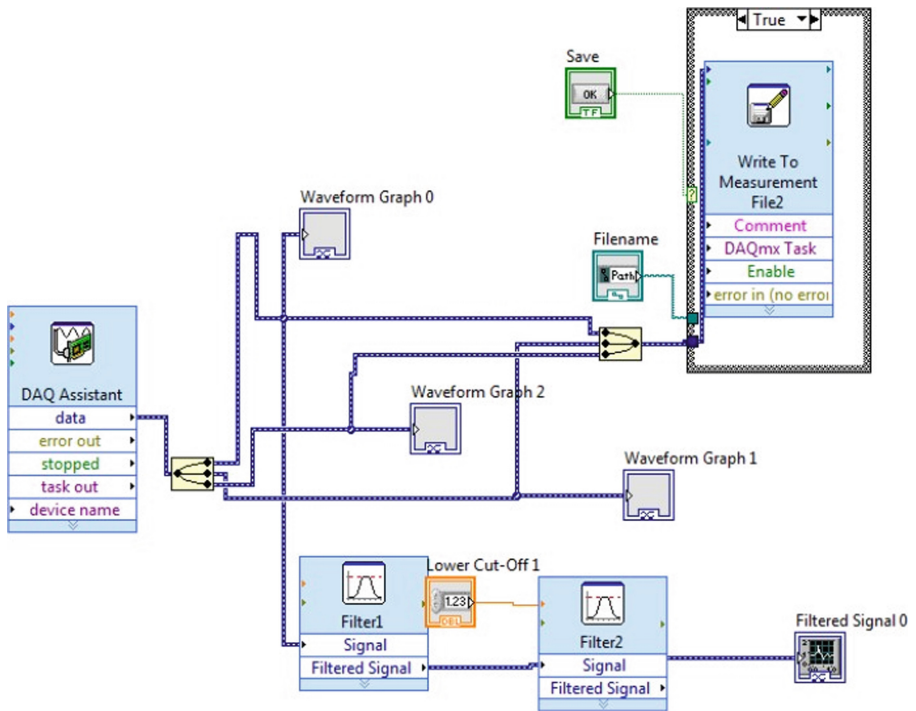


Fig. 10. Signal conditioning using LAB VIEW

PPG signal from the signal conditioning circuit is depicted in Fig. 11 using the LabVIEW waveform Graph 0 display depicted in Fig. 10.

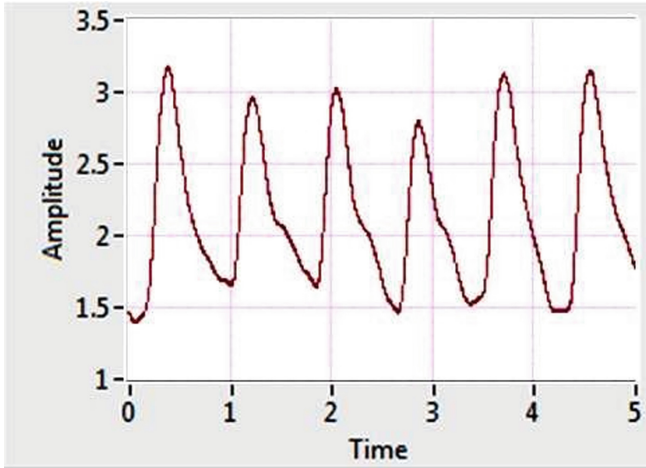


Fig. 11. PPG signal from the second stage signal conditioning circuit

In this study, to calculate heart rate and heart rate variability, first, the PPG signal has been converted into digital pulses that are close to transistor-transistor logic (TTL), as illustrated in Fig. 12. The condition of TTL outputs is often limited to narrower limits of 0.0 V to 0.4 V for a “low” and 2.4 V to VCC for a “high,” offering at least 0.4 V of noise protection. The analog PPG signal is given to Arduino pro mini analog pin A0. For this, we identify peaks in the PPG waveform when the slope of the curve changes from positive to negative and the size of the signal exceeds 80% of the threshold. So when the ADC reaches more than the threshold value, the signal will count as a pulse unless ADC values drop to 0.

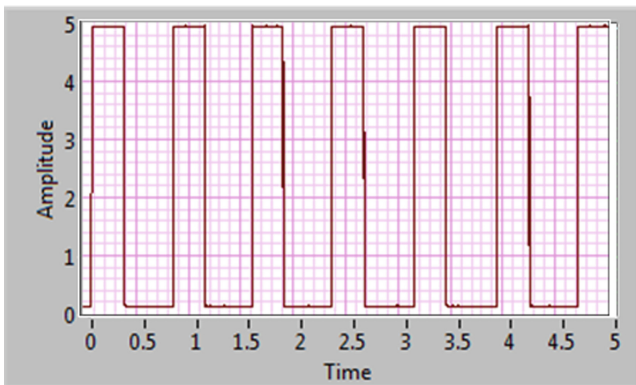


Fig. 12. TTL pulse from Arduino

2.6 Trial PPG Signal Waveform with Car

A brief test using a prototype arrangement on the car was done to determine the sensor's position. The primary goal of the test is to determine whether the PPG signal is stable and whether the heart rate varies while driving on the three body surfaces of the temple, nose, and near ear, as indicated in Fig. 13 below. As seen in Fig. 10, throughout this test, we recorded the data utilizing the LabVIEW block referred to write-to-measurement file.

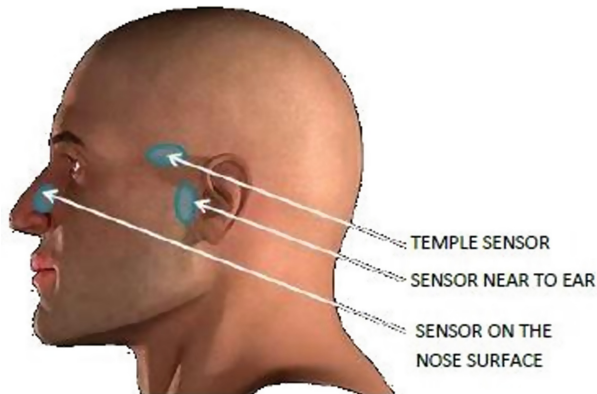


Fig. 13. Sensor position during car test

As shown in Fig. 14, the three sensors were attached to the driver's eyeglasses and signal conditioning circuit, power supply module, Bluetooth, etc. held by the back seat of the car using a breadboard, Elvis board, and laptop.



Fig. 14. Experimental test setup in the car

PPG signal from Temple Sensor

The PPG signal from the Temple sensor remained rather constant during the trial and was less impacted by the road's potholes, as seen in Fig. 15.

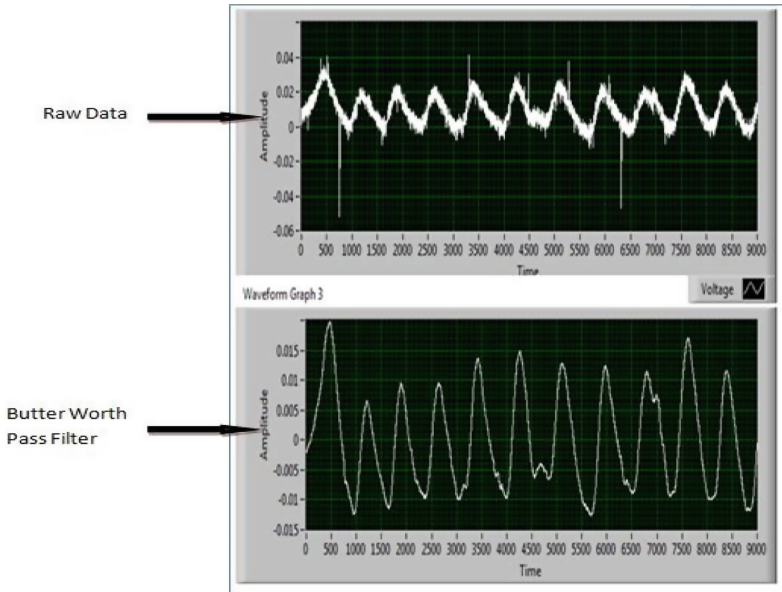


Fig. 15. PPG signal from Temple sensor

PPG signal from near Ear Sensor

According to Fig. 16, the PPG signal from the ear sensor was steady and not as significantly impacted by road imperfections. However, the sensor placed on the ear is not comfortable for continuous monitoring.

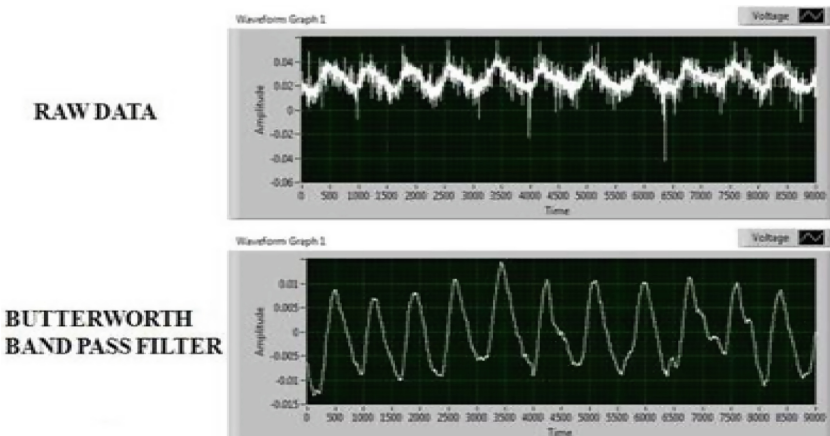


Fig. 16. PPG signal from near Ear sensor.

PPG signal from the surface of the Nose.

The PPG signal from the nose's surface is not very steady and is heavily influenced by road imperfections, as illustrated in Fig. 17.

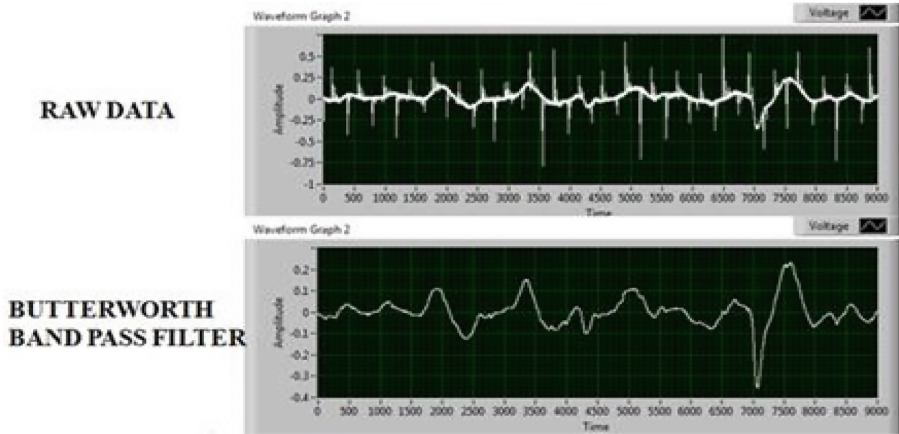


Fig. 17. PPG signal from Nose surface sensor.

2.7 Powering of the Board

In this study, a Bluetooth and Arduino board are mounted on the headband of an Intex Wireless Roaming headset, which uses two AAA batteries, each of which provides 1.5 V for sensor integration on the ear pad and holding the signal conditioning board. The maximum output voltage from these headphones is 3 V, however, we require a 5 V source to operate them. The DC-DC Boost Converter Step-Up Module 1–5 V to 5 V 500 mA is used to obtain the necessary voltage from headphones to power the board.

2.8 Printed Circuit Board (PCB) Design and Fabrication

Components have been installed on a dual-layer PCB, as shown in Fig. 18 PCB layouts, on both the component and solder sides.

Capacitor and resistor placement is on the component side, while SMD Op Amp, SMD transistor, and SMD Zener diode soldering is done on the solder side, as illustrated in Fig. 18 from left to right. This PCB has seven holes for the TP3-TP6 connector for the IR TCRT1000 sensor, 5 V, GND, and PPG output (TP7). The 5V and GND are linked to the DC-DC Boost Converter Step Up Module 1–5 V to 5 V 500 mA, TP7 is attached to the analog port (A0) of the Arduino Pro Mini, and TP3–TP6 is either directly wired or connected via a jumper to the TCRT1000 sensor (Fig. 19).

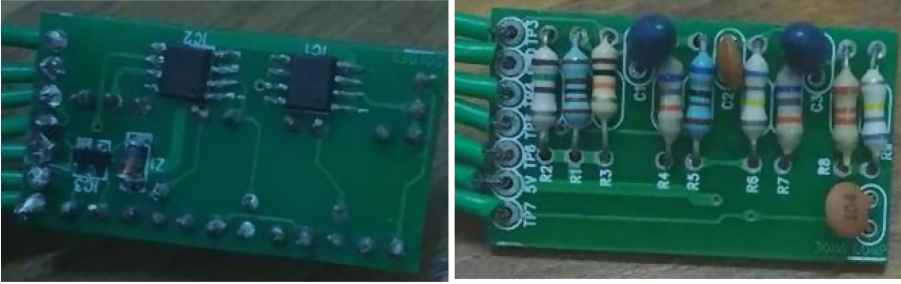


Fig. 18. Dual layers PCB of signal conditioning part

Both Bluetooth and the sensor are built into the headphone earpad and headband, respectively. Figure 20 below shows the PPG signal waveform displayed on the laptop using LabVIEW software and the heart rate displayed on the Android mobile using Bluetooth and the MIT-app Inventor app.

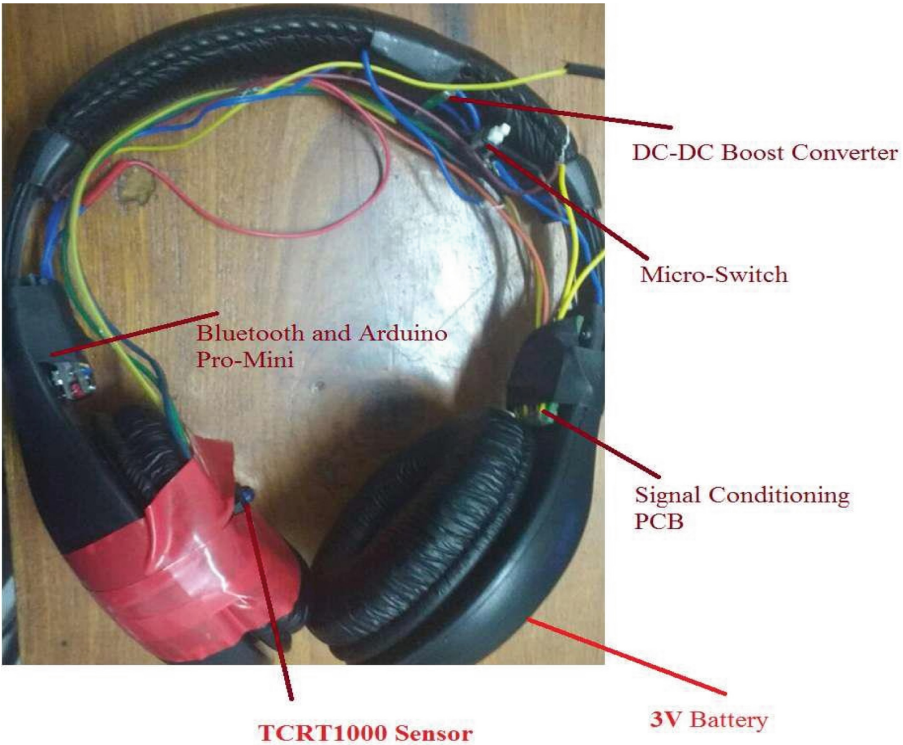


Fig. 19. Heart rate monitoring system integrate with headphones

The headphone, as shown in Fig. 20, is a component of the system; the HR and HRV are recorded without any disruption or inconvenience to the person wearing the device.



Fig. 20. Heart rate monitoring system and android display

The recorded data is wirelessly transmitted to a cellphone and displayed via Bluetooth communication.

3 Result and Discussion

3.1 Measuring the Performance of the System

Eight volunteers were used in this trial to test and validate the device's accuracy in measuring heart rate with a tolerance of ± 3 beats during a typical time of rest using WEAL's standard device, the "WEAL Pulse Oximeter Fingertip." Table 1 below displays the heart rate readings obtained from a few friends to compare to their actual heart rates.

Table 1. Heart rate readings

Subject	Age	Male/Female	Actual heart rate (bpm)	Measured heart rate (bpm)	Difference (bpm)
A	33	M	60	62	-2
B	33	M	60	63	-3
C	24	M	92	93	-1
D	25	M	76	78	-2
E	28	M	78	76	+ 2
F	25	M	78	80	-2
G	24	M	82	80	+ 2
H	28	M	90	88	+ 2

3.2 Measurements of Heart Rate Variability (HRV)

In the second phase, the heart rate variability was obtained from my heart rate at different periods of the day with fixed time intervals. To know the heart rate variation the data was recorded at hour intervals of the day. The data showed a considerable change in heart rate activeness to sleep shown in Table 2 below.

Table 2. Heart rate variation of a subject at a fixed time interval

Time	7:00 AM	9:00 AM	11:00 AM	1:00 AM	3:00 PM	5:00 PM	7:00 PM	9:00 PM	11:00 AM	1:00 AM	3:00 AM	1:00 AM
Measured HR(bpm)	84	87	84	84	90	80	81	84	83	80	75	88

3.3 Analysis of the Differences Between Measurement

In this study, Bland and Altman used a graphical method to quantify the difference between actual and measured heart rates. For the analysis, the mean of the difference in measurement methods and the standard deviation was obtained to represent mean bias and the limits of agreement. Second, the data points can be restricted using + 2 SD to demonstrate a 95% confidence interval (CI; precisely defined: mean 1.96 SD) of distributed data [17]. The mean difference (mean bias) for this measurement was -0.5, with a standard deviation of 2.13. To understand the dispersion of variables, create a scatterplot with an X-axis (average) and a Y-axis (difference). The upper limit in this study can be calculated using mean + 1.96 × SD (-0.5 + 1.96 × 2.13 = 3.69) and the lower limit using mean -1.96 × SD (-0.5-1.96 × 2.13 = -4.69). The following is an appropriate statement to use in the manuscript: The Bland-Altman plot revealed a mean bias ± SD between the first and second heart rate measurement as -0.5 ± 2.13 PBM, with the limits of agreement set at -4.69 and 3.69 (Fig. 21).

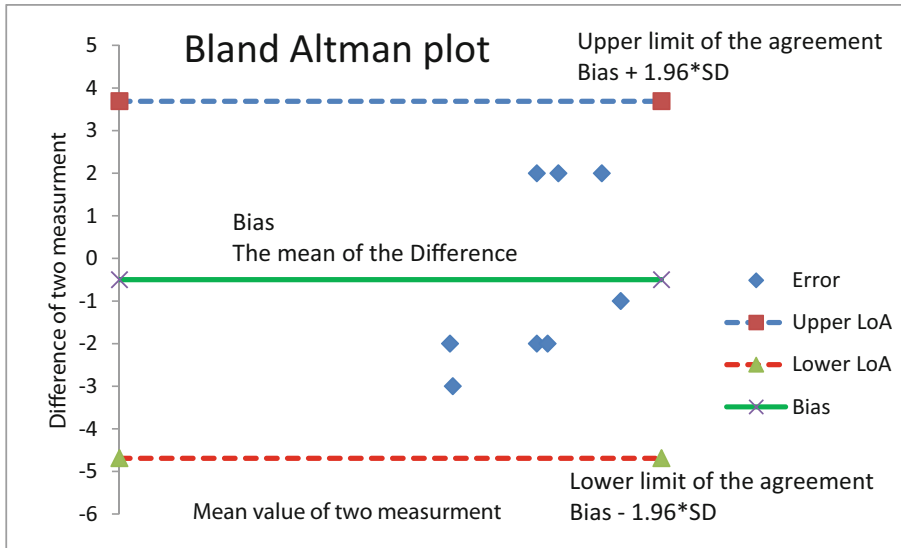


Fig. 21. Bland altman plot

4 Conclusion

This paper describes how a Reflectance PPG sensor-based heart rate monitoring system was put into practice utilizing a low-cost Pro Mini Arduino board, HC-05 Bluetooth, and other readily accessible components integrated into the headphone. Through HC-05 Bluetooth connectivity, data transmission was accomplished from the Arduino to the smartphone. A minute's worth of heartbeats are counted, and the results are displayed on an Android device using the MIT App Inventor 2 application. This product's design aims to create a tool that can serve as a personal trainer, sleepy driving detector, and anger detector. Using his or her Android phone, the motorist can monitor their level of drowsiness at any moment. Hospitals can also use this system. Here, by the suggested system, a doctor is not required to be present when the heart rate is being monitored. The patient's heart rate can be sent to the doctor remotely.

References

1. Goroso, D.G., et al.: Remote monitoring of heart rate variability for obese children. *Biomed. Signal Process. Control* **66**, 102453 (2021)
2. Shi, K., et al.: Contactless analysis of heart rate variability during cold pressure test using radar interferometry and bidirectional LSTM networks. *Sci. Rep.* **11**(1), 1–13 (2021)
3. Ma, Z., et al.: A low-power heart rate sensor with an adaptive heartbeat locked loop. In: 2021 IEEE International Symposium on Circuits and Systems (ISCAS), pp. 1–5. IEEE (2021)
4. Hinde, K., White, G., Armstrong, N.: Wearable devices are suitable for monitoring twenty-four-hour heart rate variability in military populations. *Sensors* **21**(4), 1061 (2021)
5. Vescio, B., Salsone, M., Gambardella, A., Quattrone, A.: Comparison between electrocardiographic and earlobe pulse photoplethysmographic detection for evaluating heart rate variability in healthy subjects in short-and long-term recordings. *Sensors* **18**(3), 844 (2018)

6. Prieto-Avalos, G., Cruz-Ramos, N.A., Alor-Hernández, G., Sánchez Cervantes, J.L., Rodríguez-Mazahua, L., Guarneros-Nolasco, L.R.: Wearable Devices for Physical Monitoring of Heart: a Review. *Biosensors* **12**(5), 292 (2022)
7. Shaffer, F., Ginsberg, J.P.: An overview of heart rate variability metrics and norm. *Front. Public Health* **5**, 258 (2017)
8. Chow, H.W., Yang, C.C.: Accuracy of optical heart rate sensing technology in wearable fitness trackers for young and older adults: Validation and comparison study. *JMIR Mhealth Uhealth* **8**(4), e14707 (2020)
9. Khamitkar, S.S., Rafi, M.: IoT-based system for heart rate monitoring. *Int. J. Eng. Res. Technol.* **9**(07), 1563–1571 (2020)
10. Khan, M.M., Tazin, T., Hossain, T.: Development of wireless monitoring system for pulse rate: a new approach. *Multi. Dig. Publishing Inst. Proc.* **67**(1), 13 (2020)
11. Castaneda, D., Esparza, A., Ghamari, M., Soltanpur, C., Nazeran, H.: A review on wearable photoplethysmography sensors and their potential future applications in health care. *Int. J. Biosens. Bioelectron.* **4**(4), 195 (2018)
12. Přibil, J., Přibilová, A., Frollo, I.: Comparative measurement of the PPG signal on different human body positions by sensors working in reflection and transmission modes. *Eng. Proc.* **2**(1), 69 (2020)
13. He, J., Choi, W., Yang, Y., Lu, J., Wu, X., Peng, K.: Detection of driver drowsiness using wearable devices: a feasibility study of the proximity sensor. *Appl. Ergon.* **65**, 473–480 (2017)
14. Ludwig, M., Hoffmann, K., Endler, S., Asteroth, A., Wiemeyer, J.: Measurement, prediction, and control of individual heart rate responses to exercise—Basics and options for wearable devices. *Front. Physiol.* **9**, 778 (2018)
15. Kao, Y.H., Chao, P.C.P., Wey, C.L.: Design and validation of a new PPG module to acquire high-quality physiological signals for high-accuracy biomedical sensing. *IEEE J. Sel. Top. Quantum Electron.* **25**(1), 1–10 (2018)
16. L'Her, E., N'Guyen, Q.-T., Pateau, V., Bodenes, L., Lellouche, F.: Photoplethysmographic determination of the respiratory rate in acutely ill patients: validation of a new algorithm and implementation into a biomedical device. *Ann. Intensive Care* **9**(1), 1–10 (2019)
17. Campos, L.A., Pereira, V.L., Jr., Muralikrishna, A., Albarwani, S., Brás, S., Gouveia, S.: Mathematical biomarkers for the autonomic regulation of the cardiovascular system. *Front. Physiol.* **4**, 279 (2013)
18. Doğan, N.Ö.: Bland-Altman analysis: A paradigm to understand correlation and agreement. *Turk. J. Emerg. Med.* **18**(4), 139–141 (2018)